Journal of Luminescence 130 (2010) 1160–1168

Contents lists available at ScienceDirect

Journal of Luminescence

journal homepage: www.elsevier.com/locate/jlumin

# Characterization of the interaction between human lactoferrin and lomefloxacin at physiological condition: Multi-spectroscopic and modeling description

J. Chamani [a,*], N. Tafrishi [a], M. Momen-Heravi [b]

[a] Department of Biology, Faculty of Science, Islamic Azad University—Mashhad Branch, Mashhad, Iran
[b] Department of Chemistry, Faculty of Science, Islamic Azad University—Mashhad Branch, Mashhad, Iran

ARTICLE INFO

*Article history:*
Received 9 May 2009
Received in revised form
4 February 2010
Accepted 11 February 2010
Available online 17 February 2010

*Keywords:*
Human lactoferrin
Lomefloxacin
Fluorescence quenching spectroscopy
Secondary structure
Binding constant

ABSTRACT

The interaction between lomefloxacin (LMF) and human lactoferrin (Hlf) was studied by using fluorescence, circular dichroism (CD) spectroscopic and molecular modeling measurements. By the fluorescence quenching results, it was found that the binding constant $K_A = 8.69 \times 10^5$ L mol$^{-1}$, and number of binding sites $n = 1.75$ at physiological condition. Experimental results observed showed that the binding of LMF to Hlf induced conformational changes of Hlf. The participation of tyrosyl and tryptophanyl residues of protein was also estimated in the drug–Hlf complex by synchronous fluorescence. The quantitative analysis data of far-UV CD spectra from that of the α-helix 37.4% in free Hlf to 30.2% in the LMF–Hlf complex further confirmed that secondary structure of the protein was changed by LMF. Near-UV CD showed perturbations around tryptophan and tyrosine residues which involves perturbations of tertiary structure. The thermodynamic parameters like, $\Delta H^\circ$ and $\Delta S^\circ$, have been calculated to be 63.411 kJ mol$^{-1}$ and 231.104 J mol$^{-1}$ K$^{-1}$, respectively. Thermodynamic analysis showed that hydrophobic interactions were the main force in the binding site but the hydrogen bonding and electrostatic interaction could not be excluded which in agreement with the result of molecular docking study. The distance $r$ between donor and acceptor was obtained according to fluorescence resonance energy transfer (FRET) and found to be 1.78 nm. The interaction between LMF and Hlf has been verified as consistent with the static quenching procedure and the quenching mechanism is related to the energy transfer. Furthermore, the study of molecular modeling that LMF could bind to the α-helixes between Pro145–Asn152 and Phe167–Gln172 regions and hydrophobic interaction was the major acting force for the binding site, which was in agreement with the thermodynamic analysis.



## 1. Introduction

Human lactoferrin (Hlf) has been the subject of intensive structural and functional studies since it was first isolated, simultaneously in three separate laboratories, almost 50 years ago [1–3]. Hlf, a prominent protein in several biological fluids and in the secretory granules of neutrophils, is a monomeric 80 kDa glycoprotein, with a single polypeptide chain of about 690 amino acid residues [4–6]. The defining structural feature of iron-bound (holo) Hlf is that the two domains of each lobe enclose the bound $Fe^{3+}$ ion, which is effectively sequestered away from the external environment. Four protein ligands, plus the synergistically bound $CO_3^{2-}$ anion, are covalently bound to the metal ion, which thus crosslink's the two domains that enclose it [7,8]. This explains the high stability of this structure and the difficulty of removing the bound metal without first destabilizing the protein structure, for example, at very low pH or perhaps by receptor action. It is a highly basic protein and consequently interacts with many acidic molecules [9]. Such interactions may modify the biological properties of Hlf. A wide variety of molecules of pharmacological interest have surface-active properties due to their amphiphilic nature. To achieve their target in the intracellular medium, their hydrophilic and hydrophobic moieties firstly interact with the surface of the cellular membrane and its components. This interaction plays a fundamental role for the biological phenomena. It is informative to study interaction of a tested drug with the Hlf because protein–drug binding plays an important role in pharmacology and pharmacodynamics. Information on the interaction of Hlf with drug can help us better understand the absorption and distribution of drug. Therefore, it has become an important research field in chemistry, life science and clinical medicine [10].

* Corresponding author. Tel.: +98511 8437107; fax: +98511 8424020.
*E-mail address:* Chamani@ibb.ut.ac.ir (J. Chamani).

0022-2313/$ - see front matter © 2010 Elsevier B.V. All rights reserved.
doi:10.1016/j.jlumin.2010.02.014

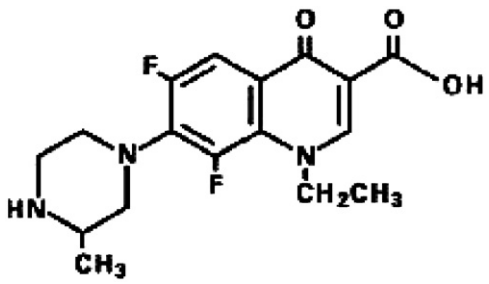


**Scheme 1.** Chemical structure of lomefloxacin.

In recent years, interaction between drugs of quinolons and protein molecules have been widely studied [11]. Quinolone derivatives, antibacterial drugs, are widely used in the chemotherapy of various infectious diseases, especially against Gram-negative bacteria, with broader spectrum and greater actively compared to nalidixic and oxolinic acid [12,13]. The medicinal functions have extensively been studied [14], and proved to prevent bacterial DNA biosynthesis by inhibiting the bacterial enzyme DNA gyrase [15,16]. In the interest of enriching the information database of such research, we chose lomefloxacin (LMF) as a donor, which is a typical representation of quinolones. LMF (Scheme 1) has been widely used clinically for the treatment of bronchitis, skin structure and urinary tract infections [17].

Due to the wide usage of phytomedicine including antibacterial fluoroquinolones for medical and health fortifying purposes, LMF has gained international popularity. However, little is known about their active principles and even less about their mechanisms of actions, which may affect the future application of this compound. In order to give a thorough understanding of absorption transport and receptor binding of these drugs at the molecular level, NMR [18], electrochemistry [19], capillary electrophoresis [20], chromatography and photometry [21–23] were ever adopted in the past decades. Some techniques commonly used to detect interaction between drug and Hlf. The binding of LMF to bovine lactoferrin in a dilute aqueous solution using fluorescence, capillary zone electrophoresis and volta metric techniques have been investigated [24–27]. Fluorescence spectroscopy is an appropriate method to study molecular interactions involving proteins because it is highly sensitive, rapid and simple. From measurements and analyses of the emission peak, the transfer efficiency of energy, the lifetime and fluorescence polarization, a vast amount of information will be obtained about the structural fluctuation and the microenvironment of the fluorophore in macromolecules. By measuring the intrinsic fluorescence quenching of Hlf, the accessibility of quenchers to the fluorophore groups of Hlf can be estimated. This information can help us predict the binding mechanisms of LMF to Hlf.

Here, the binding reaction between LMF and Hlf was investigated and the binding parameters and transfer efficiency of energy were measured. A model for this interaction is proposed where the intrinsic fluorescence of Hlf has been quenched through LMF binding by the quenching procedure. Our results may cast some light on the future study of the interaction between LMF and other proteins such as enzymes and have toxicological importance; our work should be valuable in ecotoxicology.

## 2. Materials and methods

### 2.1. Materials and solutions

All reagents used were of analytical grade and purchased from Sigma-Aldrich Co. (St. Louis, MO, USA). Hlf solution ($6.25\times10^{-6}$ M) was prepared in pH 7.40 tris–HCl buffer solution (0.05 M tris 0.1 M, NaCl). The LMF solution ($5.0\times10^{-4}$ M) was prepared by desolving in tris–HCl buffer. Water was purified with a Mill-Li-Q purification system (Barnatead, Dubuque, IA, USA) to a specific resistance $>16.4\ \mathrm{M\Omega\ cm^{-1}}$. All solution were stored in refrigerator at 4 °C in dark.

### 2.2. Apparatus

Absorbance measurements were carried out with Jasco spectrophotometer equipped with 1.0 cm quartz cells. The optical system is based on a split-beam with a grating bandwidth of 5 nm. The light source is a Xenon lamp. Fluorescence measurements were performed with a Varian Carry Eclipse fluorescence spectrophotometer (Mulgrave, Victoria, Australia) equipped with a Xenon pulse lamp and a thermostat bath. The system is based on Czerny–Turner monochromators (190–1100 nm range) supplied with a R928 photomultiplier detector (220–600 nm). The widths of both the excitation slit and emission slit were set at 5.0 nm. The operation software automatically corrects the spectral scan for the photomultiplier characteristics. Fluorescence intensities were corrected for inner filter and dilution and dilution effects before analysis of the binding and quenching data. A quartz cell of 1.00 cm was used for the measurements. Appropriate buffer has been taken blank and subtracted from the experimental spectrum to correct the background of fluorescence. All the experiments were repeated at least three times. All measurements were performed at room temperature. By scanning both the excitation and emission monochromators of a common spectrofluorometer with $\Delta\lambda=0$ nm, a resonance light scanning spectrum (RLS) can be developed, which has been proved to be able to investigate the aggregation of small molecules and the long-range assembly of drugs on biological templates. All RLS spectra were obtained by scanning simultaneously the excitation and emission monochromators (namely $\Delta\lambda=0$ nm) from 250 to 700 nm with slit widths at 5 nm for the excitation and emission. The synchronous fluorescence spectra were obtained by scanning simultaneously the excitation and emission monochromators. The synchronous fluorescence spectra only show the tyrosine and tryptophan residues of Hlf when the wavelength interval ($\Delta\lambda$) is 15 nm and 60 nm, respectively.

Far-UV CD and near-UV CD experiments were performed on a Jasco-815 spectropolarimeter equipped with a Jasco 2-syringe titrator. Spectra were recorded with protein concentrations $6.25\times10^{-6}$ M in a 1-mm path length quartz cuvette. A bandwidth of 1 nm and a response of 2 s were used, with a scanning rate at $50\ \mathrm{nm\ min^{-1}}$ to obtain final spectra as an average of four scans. The instruments were calibrated with ammonium d-10-camphorsulfonic acid. The induced ellipticity was obtained by the ellipticity of the drug–Hlf mixture subtracting the ellipticity of drug at the same wavelength and is expressed in degrees. The results are expressed as the mean residue ellipticity [$\theta$], which is defined as $[\theta]=100\times\theta_{\mathrm{obsd}}/(\mathrm{LC})$, where $\theta_{\mathrm{obsd}}$ is the observed ellipticity in degrees, *C is* the concentration in residue $\mathrm{mol\ cm^{-3}}$ and $l$ is the length of the light path in cm. All pH measurements were made with a Metrom digital pH-meter (Metrom, Germany).

### 2.3. Procedures

Hlf and LMF were dissolved in tris–HCl buffer, the concentrations of Hlf and LMF were $6.25\times10^{-6}$ and $5\times10^{-4}$ M, respectively. To a 1.0 cm quartz cell, Hlf solution was added to make up 2.5 ml and the range of the drug solution was gradually titrated manually into the cell using a micro-injector. The fluorescence spectra were then

measured (excitation at 280 and 295 nm and emission wavelengths of 290–600 nm) at room temperature. Both entrance slit and exit slit width being 5 nm and scanning speed of 240 nm/min, fluorescence quenching spectra and synchronous fluorescence spectra were obtained. The UV/vis absorbance spectra of Hlf and LMF were recorded at 291 nm at room temperature. The far-UV and near-UV CD spectra of Hlf and LMF were read and spectral scanning curves were made at the same condition.

## 3. Results and discussion

### 3.1. Fluorescence properties of Hlf by LMF

For macromolecules, the fluorescence measurements can give some information of the binding of small molecule substances to protein on the molecular level, such as the binding mechanism, binding mode, binding constant, intermolecular distances, etc. Fluorescence quenching is the decrease of the quantum yield of fluorescence from a fluorophore induced by a variety molecular interactions with quencher molecule, such as excited-state reaction, molecules rearrangement, energy transfer, ground state complex formation and collision quenching [28,29].

The different mechanisms of quenching are usually classified as either dynamic quenching or static quenching. Dynamic quenching refers to a process that the fluorophore and the quencher come into contact during the transient existence of the excited state. Static quenching refers to fluorophore–quencher complex formation. In general, dynamic and static quenching can be distinguished by their different dependence on temperature and viscosity, or by the difference of their fluorescence lifetime [30]. Participitation of tyrosine and tryptophan groups in LMF–Hlf complexes is assessed using different excitation wavelengths. At 280 nm wavelength the tryptophanyl and tyrosyl residues in Hlf are excited, whereas the 295 nm wavelength excites only tryptophanyl residues. At 295 nm wavelength, the absorbances of tyrosine residues reduce by acryl amide and iodide and also minimize the fluorescence and radiationless energy transfer from tyrosine residues. Comparison of fluorescence quenching of protein excited at 280 and 295 nm allows estimating the participitation of tryptophan and tyrosine groups in the complex [31].

Fig. 1 shows the fluorescence quenching spectra of the free Hlf induced by different concentrations of LMF. It is obvious that Hlf has a strong fluorescence emission peaked at 328 nm after being excited with a wavelength of 280 and 295 nm. When a fixed concentration of Hlf was titrated with different amounts of LMF, a remarkable fluorescence decrease of Hlf was observed. It can also be noticed from the spectra that the interaction of Hlf with LMF led to a slight blue shift at the maximum wavelength of Hlf fluorescence emission, especially at high drug concentration, which indicated that the chromophore of protein has been brought to a more hydrophobic environment and the conformation of the protein has been changed [32–34]. The quenching takes place when the quencher is sufficiently close to the tryptophanyl or/and tyrosyl residues. Then the energy transfer between a ligand and fluorophore is possible. The quenching of Hlf fluorescence may be considered as a result of the formation of LMF–Hlf complex. Fig. 2 shows the fluorescence quenching of protein excited at 280 and 295 nm wavelength do not overlap. This phenomenon shows that in the interaction of LMF with Hlf, both the tryptophanyl and tyrosyl groups take part. The quenching curves of Hlf excited at 280 and 295 nm in the presence of LMF overlap below the molar ratio LMF/Hlf, 2/1 and do not overlap above it. It means that when there are fewer than 2 LMF molecules for 1 Hlf molecule, only tryptophanyl residues take part in the interaction, whereas above this number of LMF molecules tryptophanyl and tyrosyl residues participate in it.

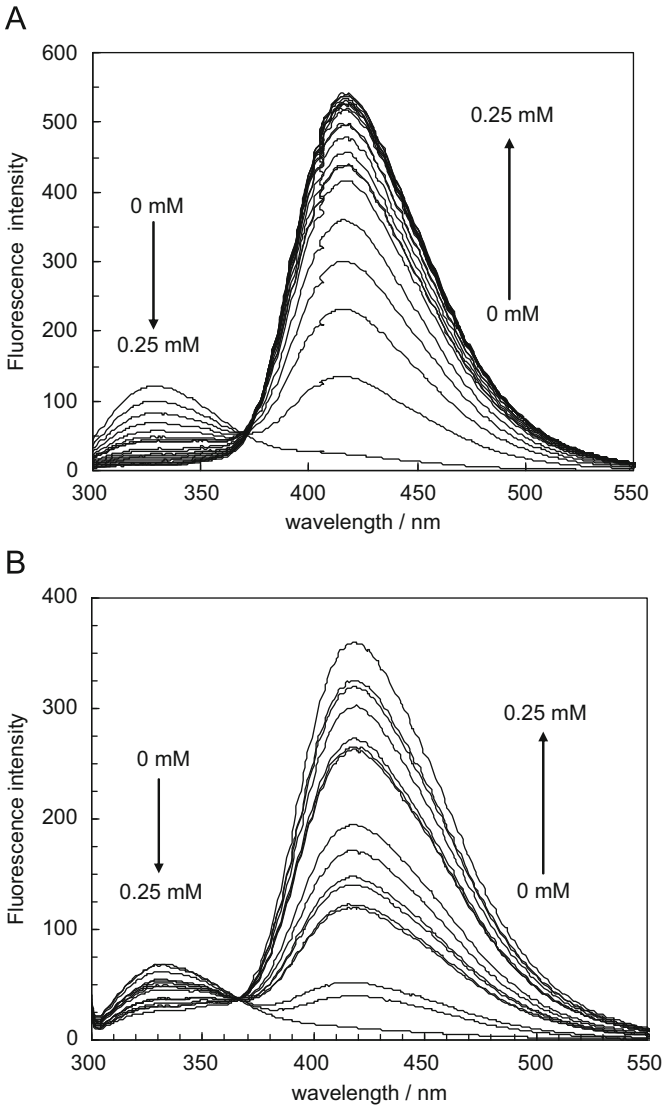


**Fig. 1.** Fluorescence emission spectra of Hlf–LMF system. The concentration of Hlf was $6.25 \times 10^{-6}$ M and LMF concentration was increased from (0 to 2.5) $\times 10^{-4}$ M. $T$=298 K; pH 7.40, (A) $\lambda_{ex}$=280 nm; (B) $\lambda_{ex}$=295 nm.

The fluorescence quenching behaviour could be analyzed using the Stern–Volmer [35–37] and Lehrer [38] equations for linear and non-linear (hyperbolic) fittings, respectively. Dynamic quenching is described by the well known Stern–Volmer equation

$$F_0/F = 1 + K_{SV}[Q] \quad (1)$$

where $F_0$ and $F$ are the relative fluorescence intensities of Hlf at 328 nm in the absence and presence of quencher, [$Q$] is the quencher concentration and $K_{SV}$ is the Stern–Volmer dynamic quenching constant. In some situations the Stern–Volmer plot presents negative divergences from linearity, following a hyperbolic-like behaviour. In general, these situation result from the existence of more than one class of fluorophores (e.g., different tryptophan residues subpopulations in proteins), with different $K_{SV}$ values. The simplest situation considers the existence of a fluorophore population A protected from contact with the quencher, and a population B accessible to it. In this case, the fluorescence data can be analyzed using the Lehrer equation [38]

$$F_0/F = 1 + K_{SV}[Q]/(1 + K_{SV}[Q])(1 - f_B) + f_B \quad (2)$$

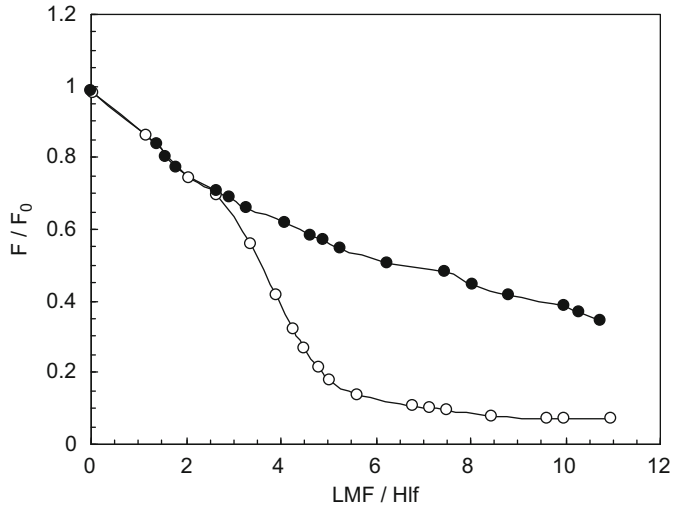


**Fig. 2.** Quenching curves of Hlf in the presence of LMF. $T$=298 K; pH=7.40. $\lambda_{ex}$=280 nm (○); $\lambda_{ex}$=295 nm (●). The error calculated as maximum deviation does not exceed the symbols.

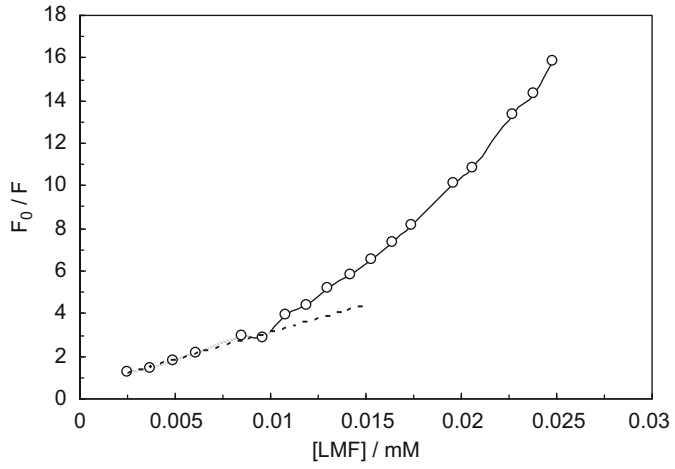


**Fig. 3.** Stern–Volmer curve of Hlf fluorescence quenching treated with different concentrations of LMF in the drug to protein molar ratios ranged from 0.322 to 0.98. Hlf concentration was $6.25\times10^{-6}$ M, $\lambda_{ex}$=280 nm; $T$=298 K.

where

$$f_B = F_{0,B}/F_0 \quad (3)$$

and $F_{0,B}$ is the fluorescence intensity of the fluorophore population accessible to the quencher. When both subpopulations (accessible and non-accessible) have identical quantum yields, the $f_B$ value represents the mole fraction of the accessible population. The values of $K_{SV}$ were calculated from the slope of $F_0/F$ versus [Q] when a linear behaviour was observed (Eq. (1)). For hyperbolic behaviours, $K_{SV}$ and $f_B$ values were obtained from non-linear fits to Eq. (2).

Fig. 3 shows the quenching of tryptophan emission with LMF concentration recorded at 328 nm after excitation at 280 nm wavelength. Although LMF has fluorescence emission peak at about 380–550 nm, its emission in the range (320–380) nm was negligible. Nevertheless, to neglect completely its contribution, spectra were taken using reference solutions with the same drug concentration than those used in the binding experiments. Drug binding to the protein shows two regions in the mole ratio analyzed as occurred for the interaction of other ligands to protein [39–41]. The first region involves a decrease in fluorescence induced by drug binding at LMF/Hlf mole ratios up to 0.98 with a linear form. This decrease is quite important which might denote an structural modification of Hlf in such a way that tryptophan residues of Hlf located in a more hydrophilic environment [42,43]. Linear Stern–Volmer plot may either reveal the occurrence of just binding site for quencher in the proximity of the fluorophore, or indicate the existence of a single type quenching. The curve was not linear when drug to protein mole ratios were higher than 0.98. The linear region Stern–Volmer plot, fitted using the Stern–Volmer (Eq. (1)), while the hyperbolic region Stern–Volmer plot fitted by using the Lehrer equation (Eq. (2)). According to Eq. (1) the curve of $F_0/F$ versus [Q] at low concentrations of LMF was plotted. However, the Stern–Volmer curve was not linear when the LMF/Hlf concentration ranged from 1.4 to 43.9 and it showed upward curvature toward $y$ axis at high drug concentrations (see Fig. 3). The regression equation was obtained in the linear range ([LMF]/[Hlf]) from 0.322 to 0.98, $y=(0.56\pm0.032)+(2.53\pm0.12)\times10^5Q$ ($R$=0.9998, $n$=1.75). The Stern–Volmer quenching constant was calculated from the slope of the regression curve, $K_{SV}=2.54\times10^5$ L mol$^{-1}$. The biomolecular quenching rate constant was obtained from $K_{SV}$, $k_Q=2.54\times10^{12}$ L mol$^{-1}$ s$^{-1}$. It can be seen that $k_Q$ is largely higher than the limiting diffusion constant $K_{dif}$ of the biomolecule ($K_{dif}=2.0\times10^{10}$ L mol$^{-1}$ s$^{-1}$) [42,43], which suggested that the fluorescence quenching was caused mainly arisen from static quenching by complex formation [44,45]. At higher drug concentrations, the deviation from the linearity of the Stern–Volmer plot indicated that both dynamic and static quenching was involved as discussed in the literature [44,45]. The observation that there was interaction occurring between Hlf and LMF and that tryptophan residues were quenched with similar affinities suggests two simultaneous modes of interaction: (i) LMF molecules bind within the hydrophobic pockets of Hlf and (ii) they surround the Hlf protein. On the other hand, LMF-induced fluorescence quenching results were analyzed to obtained several binding parameters, then the equilibrium between free and bound molecule could be given by the following equation [46–49]:

$$\log[(F_0-F)/F] = \log K_A + n\log[Q] \quad (4)$$

where $K$ was the binding constant, reflecting the degree of Hlf and LMF; $n$ was the number of binding sites, specifying the number of LMF bound to a Hlf macromolecules. From a plot of $\log[(F_0–F)/F]$ versus $\log[Q]$, $n$ and $K_A$ were derived by fitting the linear region. $K_A$ and $n$ values obtained $8.69\times10^5$ L mol$^{-1}$ and 1.75 at physiological condition, respectively (see Fig. 4). Table 1 shows the binding constants, $K_A$ and binding sites, $n$, for LMF associated with Hlf at three different temperatures. The results determined that the binding constants were decreased with the temperature, which may indicate forming an unstable compound. The unstable compound would be partly decomposed with the rising temperature, therefore the values of $K_A$ decreased. The values of $n$ approximately equal to 1.75 indicated the existence of two binding site in Hlf for LMF; there are two certain fractions of the protein in the solution capable of binding the ligand.

The interaction forces between a drug and a biomolecule may include hydrophobic force, electrostatic interactions, vander Waals interactions, hydrogen bonds, etc. [50,51]. To obtain such information, the implications of the present results have been discussed in conjunction with thermodynamic characteristics obtained for LMF binding and the thermodynamic parameters were calculated from the Vant Hoff equation. From Table 1, it can be seen that the negative sign for $\Delta G^\circ$ indicates the spontaneity of the binding of LMF with Hlf [52]. $\Delta H^\circ$ and $\Delta S^\circ$ are positive values. According the views of Timasheff [53] and Ross and Subramanian [54], the positive $\Delta H^\circ$ and $\Delta S^\circ$ values are associated with hydrophobic interaction. The positive $\Delta H^\circ$ and $\Delta S^\circ$ values of the interaction of LMF and Hlf indicate that the binding is mainly entropy driven and the enthalpy is unfavourable for it, the hydrophobic forces playing a major role in the binding.

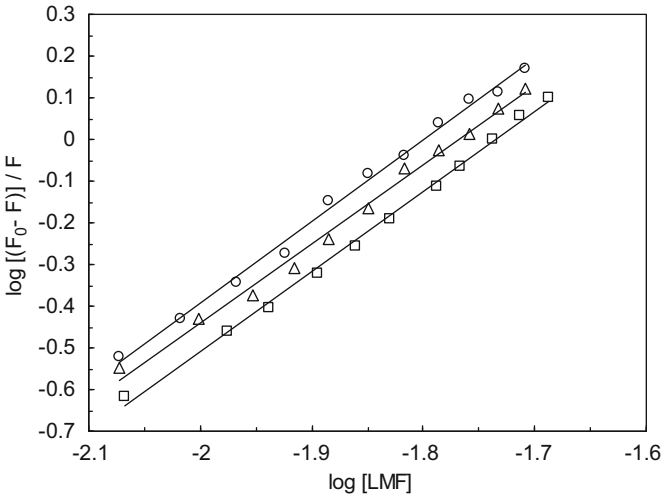


**Fig. 4.** The Hill plots of the Hlf–LMF at different temperature (○, 298 K; Δ, 310 K; □, 318 K). [Hlf]=6.25 × 10$^{-6}$ M, pH 7.40, $\lambda_{ex}$=280 nm.

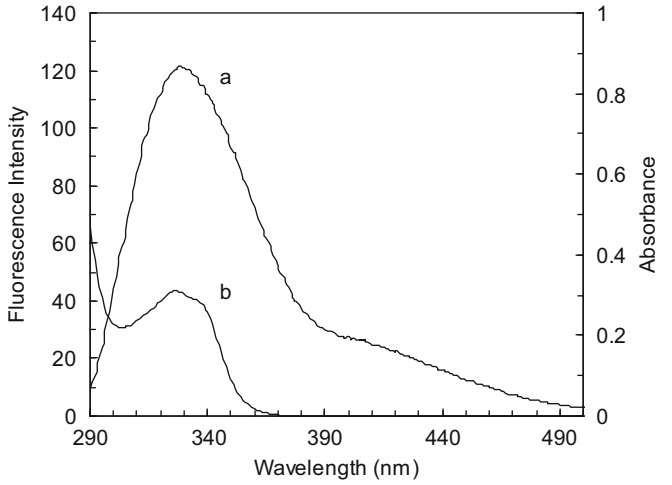


**Fig. 5.** Spectral overlap of the fluorescence spectra of Hlf (a) with the absorption spectra of LMF (b). [Hlf]=[LMF]=6.25 × 10$^{-6}$ M.

**Table 1**
Thermodynamic parameters of LMF–Hlf interaction at pH 7.40.

| $T$ (K) | $K_A$ ( × 10$^{-5}$ L mol$^{-1}$) | $n$ | $R$ | SD | $\Delta H^\circ$ (kJ mol$^{-1}$) | $\Delta G^\circ$ (kJ mol$^{-1}$) | $\Delta S^\circ$ (J mol$^{-1}$ K$^{-1}$) |
|---|---|---|---|---|---|---|---|
| 298 | 8.69 | 1.75 | 0.9998 | 0.0150 | 63.411 | −33.881 | 231.104 |
| 310 | 6.57 | 1.73 | 0.9995 | 0.0088 | | −34.524 | |
| 318 | 4.79 | 1.72 | 0.9993 | 0.0063 | | −34.580 | |

$R$ is the correlation coefficient.
SD is the standard deviation.

### 3.2. Energy transfer from Hlf and LMF

According to Forster's non-radiative energy transfer theory [55], if the emitted fluorescence from donor could be absorbed by an acceptor, energy may transfer from the donor to the acceptor. The fluorescence quenching of Hlf after binding to LMF indicated the transfer of energy between LMF and Hlf occurred. The energy transfer effect is related not only to the distance between the acceptor and the donor, but also to the critical energy transfer distance. The distance between the donor (Hlf) and the acceptor (LMF) can be calculated according to the Forster's non-radiative energy transfer theory. The efficiency of energy transfer, $E$, is described by the following equation:

$$E = 1 - F/F_0 = R_0^6/(R_0^6 + r^6) \quad (5)$$

where $F$ and $F_0$ are the fluorescence intensities of Hlf in the presence and absence of LMF, $r$ the distance between acceptor and donor and $R_0$ the critical distance when the transfer efficiency is 50%

$$R_0^6 = 8.8 \times 10^{-25} K^2 N^{-4} \Phi J \quad (6)$$

where $K^2$ is the spatial orientation factor of the dipole, $N$ the refractive index of the medium, $\Phi$ the fluorescence quantum yield of the donor, $J$ the overlap integral of the fluorescence emission spectrum of the donor and the absorption spectrum of the acceptor (Fig. 5) which can be calculated by the equation

$$J = (\Sigma F(\lambda)\varepsilon(\lambda)\lambda^4\ \Delta\lambda)/\Sigma F(\lambda)\ \Delta\lambda \quad (7)$$

$F(\lambda)$ is the fluorescence intensity of the fluorescence donor at wavelength $\lambda$, and $\varepsilon(\lambda)$ the molar absorption coefficient of the acceptor at wavelength $\lambda$. The overlap integral $J$ can be evaluated by investigating the spectra in Fig. 5 in this paper, $J$ is given by the following Eq. (7) and was calculated to be 6.83 × 10$^{-15}$ (cm$^3$ dm$^3$)/mol for Hlf. Under these experimental conditions, the distance corresponding to 50% energy transfer from Hlf to LMF can be estimated to be $R_0$=3.2 nm from Eq. (6) using $K^2$=2/3, $N$=1.36, $\Phi$=0.13 [56]. Moreover, the energy transfer effect is $E$=0.180 for Hlf from Eq. (5) and the binding distance between LMF and amino acid residues in Hlf is $r$=1.78 nm. So the distance between LMF and tryptophan residues in Hlf is 1.78 nm, which is far lower than 7 nm [57]. This obeys the conditions of Foster energy transfer theory.

### 3.3. Conformation investigation

The synchronous fluorescence spectra present the information about the molecular microenvironment in the vicinity of the fluorophore functional groups, and have several advances, such as sensitivity, spectral simplification, spectral bandwidth reduction and avoiding different perturbing effects [58]. When the $D$-value ($\Delta\lambda$) between excitation wavelength and emission wavelength were set at 15 or 60 nm, the synchronous fluorescence can provide the characteristic information of tyrosine and tryptophan residues in protein, respectively [59]. The effect of LMF on Hlf synchronous fluorescence spectroscopy is shown in Fig. 6. It is apparent from Fig. 6 that the emission maximum of tyrosine residues did a little red shift and the significant blue shift of tryptophan residues fluorescence, which indicated that the conformation of Hlf was changed, the polarity around the tyrosine residues was increased and the hydrophobicity was decreased, while the polarity around the tryptophan residues was decreased and the hydrophobicity was increased [60]. It has been also shown in Fig. 7 that the slope was higher when $\Delta\lambda$ was 60 nm indicating that a significant contribution of tryptophanyl residues in the fluorescence of Hlf, LMF was closer to tryptophan residues compared to tyrosine residues at the protein. Therefore, the binding of LMF to Hlf probably induces the tertiary structural

changes of the adsorbed Hlf and produces perturbation of microenvironments around aromatic amino acid residues. Besides the conformational changes of the protein, the energy transfer process between tryptophan is more than tyrosine; therefore fluorescence of tryptophan compared to tyrosine becomes the main luminescent species, leading to relatively larger blue shifts. The RLS spectra of Hlf, Hlf–LMF complex are recorded by synchronous scanning from 200 to 700 nm with $\Delta\lambda=0$ nm (data are not shown). The Hlf has very weak RLS signals, in contrast, a strong broad RLS band can be observed for the mixture of LMF and Hlf, indicating that the interaction between LMF and Hlf has occurred. The production of RLS is correlated with the formation of certain aggregation and the RLS intensity is dominated primarily by the particle dimension of the formed aggregation in solution [61,62]. Bearing these points in mind, it is inferred from the results that the added LMF may interact with Hlf in solution, forming a new Hlf–LMF complex that could be expected to be an aggregate. Based on these experimental results, a conclusion can be drawn that the

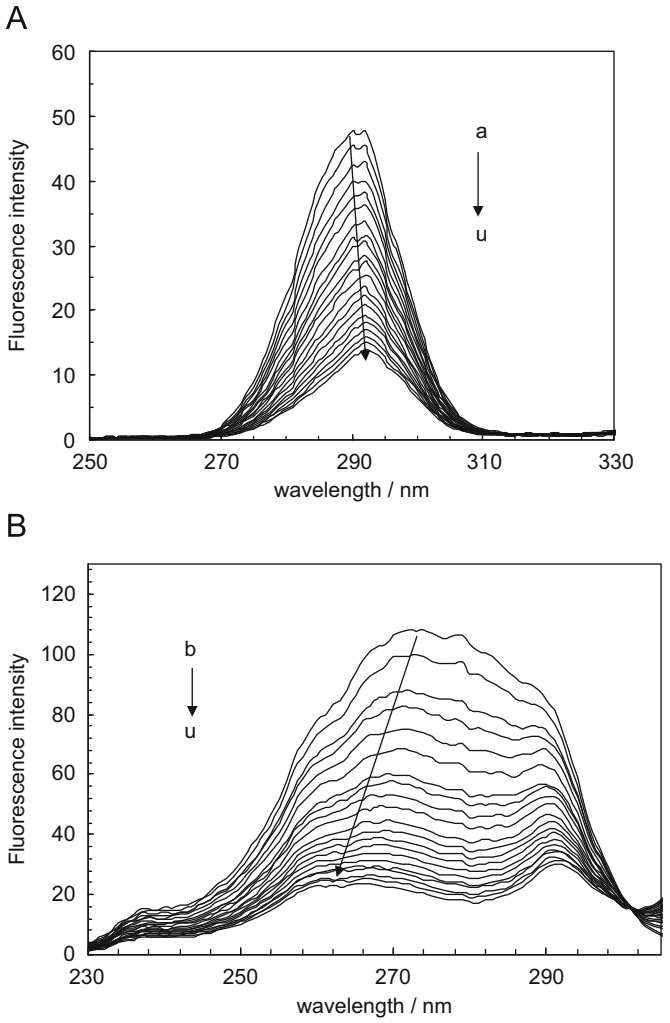


**Fig. 6.** The synchronous fluorescence spectra of Hlf in the present of LMF ($T=298$ K; pH 7.40). (A) $\Delta\lambda=15$; (B) $\Delta\lambda=60$. (a) $6.25\times10^{-6}$ M Hlf; (b→u) shows LMF concentrations from $10^{-3}$ to $20\times10^{-3}$ mM.

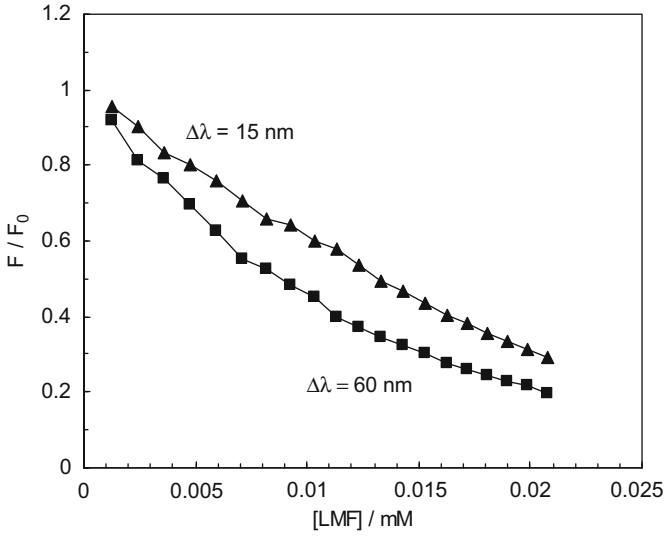


**Fig. 7.** The quenching of Hlf synchronous fluorescence by LMF. The concentration of Hlf was $6.25\times10^{-6}$ M. (▲) $\Delta\lambda=15$ and (■) $\Delta\lambda=60$ nm.

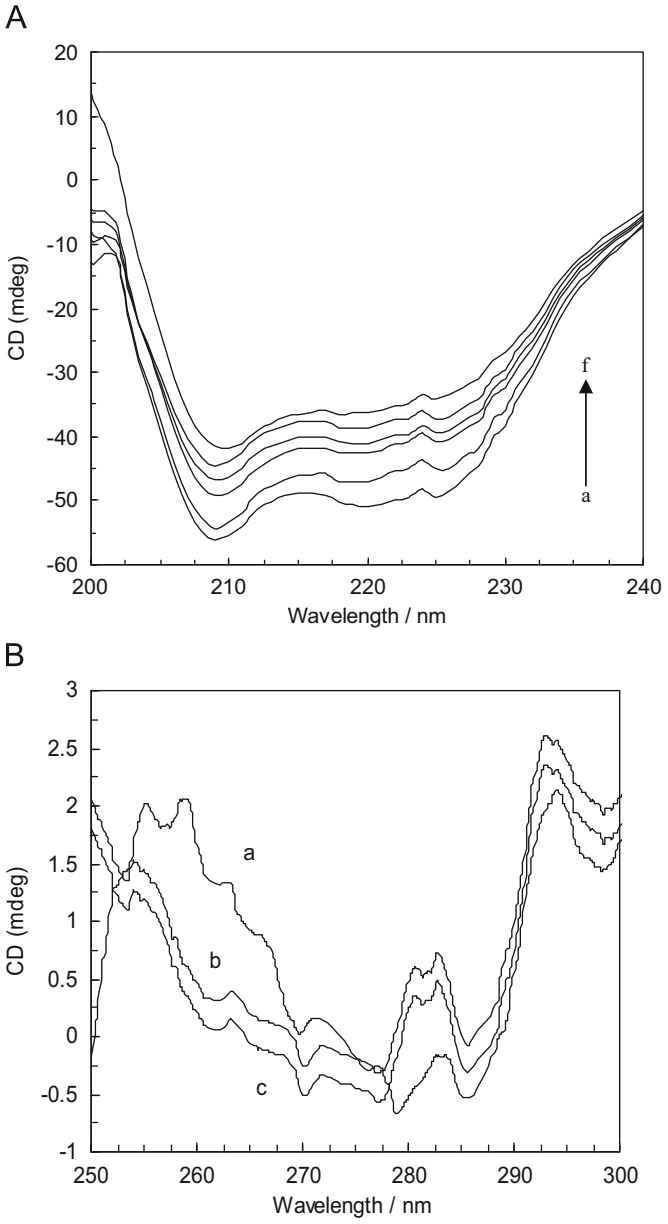


**Fig. 8.** (A) Far-UV CD and (B) near-UV CD spectra of Hlf in absence and presence of LMF at pH 7.40 and $T=298$ K. [Hlf]$=6.25\times10^{-6}$ M. LMF concentrations for Hlf–LMF system (from a to f) was 0 to $20\times10^{-3}$ mM at far-UV CD. At near UV-CD spectra, (a) Hlf in the presence of 0 mM LMF, (b) Hlf in the presence of $10^{-3}$ mM LMF and (c) Hlf in the presence of $2\times10^{-3}$ mM.

**Table 2**
Fractions of secondary structure of Hlf in the absence and presence of LMF at different temperature (pH=7.40).

| $T$ (K) | System | $f_\alpha$ | $f_\beta$ | $f_T$ | $f_U$ |
|---|---|---|---|---|---|
| 298 | Hlf | 37.4 | 28.2 | 15.8 | 18.6 |
| | Hlf–LMF | 30.2 | 28.9 | 15.1 | 25.8 |
| 310 | Hlf | 36.7 | 29.3 | 12.8 | 21.2 |
| | Hlf–LMF | 27.1 | 30.1 | 14.5 | 28.3 |
| 318 | Hlf | 33.8 | 30.4 | 11.7 | 24.1 |
| | Hlf–LMF | 25.4 | 27.9 | 15.3 | 31.4 |

$f_\alpha$, $f_\beta$, $f_T$ and $f_U$ are the fractions of α-helix, β-sheet, turn and unordered coil.

tryptophan and tyrosine residues quenching by LMF have two simultaneous modes of interaction including the LMF molecules via the hydrophobic interaction entering the hydrophobic cavity of Hlf and aggregating at its surface.

To confirm how the protein structure is changed upon drug binding, changes in chirality are a good indication of ongoing folding changes and especially of tertiary and secondary structure modifications. Thus LMF-induced conformational transitions of Hlf were monitored by far-UV and near-UV CD spectroscopy at different drug concentrations. The CD spectrum of Hlf exhibits two negative bands about 208 and 222 nm (Fig. 8(a)), which are characteristics of a high α-helical content [63,64]. The values of

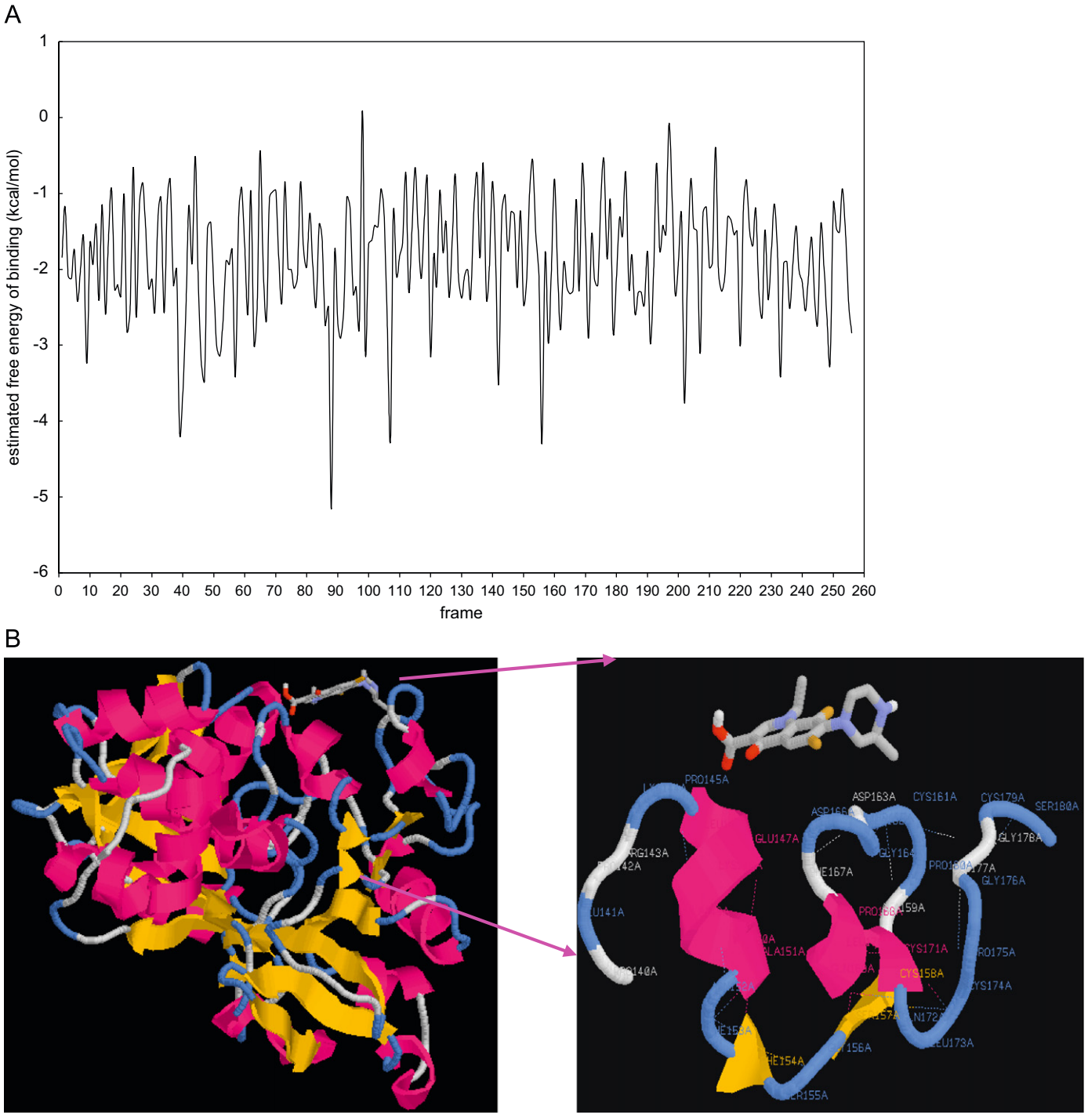


**Fig. 9.** (A) Estimated Gibbs free energy of binding values between LMF and Hlf interaction. (B) The interaction mode between LMF and Hlf (residues 140–180). The hydrogen bond between LMF and Hlf is represented using dashed line.

the negative peaks at $[\theta]_{208}$ and $[\theta]_{222}$ slightly decrease the mole ratio values of 0.98, which denotes the secondary structure is not greatly affected in this drug concentration range. At higher ratios, a more sevre decrease of the ellipticity is noted which arises from an unfolding process underwent by the protein in the presence of excess drug molecules. The fractions of α-helix, β-sheet, turn and unordered coil were then estimated by SELCON3, with 43 mode proteins with known precise secondary structures used as the reference set [64], and the results are shown in Table 2. The α-helical content decrease from 37.4% to 30.2%; the content of unordered coil increases from 18.6% to 25.8% at 298 K. A decrease in α-helical content and an increase in unordered coil structures were observed with the adsorbed Hlf. The results suggest that the Hlf molecules probably adopt a looser conformation with the extended polypeptide structures. The conformational transition probably results in the exposure of the hydrophobic cavities and a perturbation of microenvironments around the deprotonated aromatic amino acid residues, which are favourable for the Hlf adsorption onto the surface of LMF. Near-UV CD is a powerful tool for probing protein tertiary structures. The near-UV CD spectrum obtained featured one broad negative band with two minima at 285 and 278 nm (Fig. 8(b), dashed line), which correspond to the measured absorption bands. These reflect the transition of the tyrosine's phenyl ring from the ground state to the zeroth and first vibrational level of the $L_b$ excited state (0–0 and 0–1 transitions) [65,66]. Similarly, the pronounced features at 271 and 263 nm are typical for the 0–0 and 0–1 transitions of the phenylalanine's $L_b$ state. By increasing the mole ratio of LMF/Hlf, the ellipticity becomes progressively less negative that denotes perturbation around the tryptophan and tyrosine residues [67], which involves appreciable perturbations of tertiary structure.

### 3.4. Molecular modeling of the LMF–Hlf complex

The experimental observations were followed up with docking studies where LMF was docked to Hlf to determine the preferred binding site on the protein. The crystal structure of Hlf was taken from the Brookhaven Protein Data Bank (entry codes 1BTJ). The potential of the 3-D structure of Hlf was assigned according to the Amber 4.0 force field with Kollman-all-atom charges. The initial structure of the LMF was generated by molecular modeling software Vegga zz [68]. The geometrics of the molecules were subsequently optimized to minimal energy using the Tripos force field with Gasteiger–Marsili charges [69]. At last, Autodock 4 program was used to establish the interaction modes between LMF and Hlf [70]. Lamarckian genetic algorithm (LGA) program was used to calculate conformational possibility between LMF and Hlf. Fig. 9(A) and (B) exhibit the optimal energy ranked result of LMF interaction with the residues of Hlf and the LMF–Hlf conformation. The interaction between LMF and Hlf was not exclusively hydrophobic in nature since the several ionic and polar residues in the proximity of the ligand play important roles in stabilizing the negatively charged LMF molecule via H-bonds and electrostatic interactions. From Fig. 9, it can be seen that LMF binds between two α-helix regions (α-helix residues Pro145-Asn152 and α-helix residues Phe167-Gln172). Then LMF can be bound to Hlf with the effect on two α-helixes which was in agreement with the far-UV CD curves. The calculated binding Gibbs free energy ($\Delta G^\circ$) is $-23.527\ \mathrm{kJ\ mol^{-1}}$, which was not very close to the experimental data ($-30.834\ \mathrm{kJ\ mol^{-1}}$) in some degree. A possible explanation may be that the X-ray structure of the protein from crystals differs from that of the aqueous system used in this study.

## 4. Conclusion

The interaction between LMF and Hlf has been investigated in this work using different spectroscopic and molecular modeling techniques. The change on the protein conformation upon binding was followed as a function of added drug by fluorescence and CD spectroscopy. The distance $r=1.78$ nm between Hlf and LMF was obtained according to fluorescence resonance energy transfer. Changes in the environment of the aromatic residues are also observed by synchronous fluorescence and near-UV CD. The results indicated that the structure of Trp and Tyr residues environments was altered and physiological functions of Hlf were affected by LMF. It was showed that the fluorescence of Hlf has been quenched for reacting with LMF and forming a certain kind of new compound. This study shows that the fluorescence quenching technique could provide a promising tool to study the interaction of organic drugs and proteins. The results indicate that the fluorescence quenching mechanism for Hlf through LMF binding is static and dynamic quenching process at low and high concentration of drug, respectively. The binding reaction of LMF with Hlf is spontaneous and is largely mediated by hydrophobic forces. This study is expected to provide important insight into the interactions of the physiological important protein with LMF.

## Acknowledgment

The financial support of the Research Council of the Islamic Azad University-Mashhad Branch is gratefully acknowledged. The authors thank Mrs. Gile for the English editing.

## References

[1] M.L. Groues, J. Am. Chem. Soc. 82 (1960) 3345.
[2] B. Johnson, Acta Chem. Scand. 14 (1960) 510.
[3] J. Montreuil, J. Tonnelat, S. Mullet, Biochim. Biophys. Acta 45 (1960) 413.
[4] M.R. Eftink, C.A. Ghiron, Biochemistry 15 (1976) 672.
[5] P.L. Masson, J.F. Heremans, E. Schonne, J. Exp. Med. 130 (1969) 643.
[6] R.M. Bennett, A.C. Eddie-Quartey, P.J.L. Holt, Arthritis Rheumat. 16 (1973) 186.
[7] E.N. Baker, Adv. Inorg. Chem. 41 (1994) 389.
[8] B.F. Anderson, H.M. Baker, G.E. Norris, D.W. Rice, E.N. Baker, J. Mol. Biol. 209 (1989) 711.
[9] F. Lampreave, A. Pineiro, J.H. Brock, H. Castillo, L. Sanchez, M. Calvo, Int. J. Biol. Macromol. 12 (1990) 2.
[10] G. Zhang, Q. Que, J. Pan, J. Guo, J. Mol. Struct. 881 (2008) 132.
[11] X. Chen, J.C. Fan, Y. Wang, C.P. Fan, Z.C. Shang, Anal. Sci. 22 (2006) 427.
[12] J.R. Prous, N.E. Mealy, Drugs Today 19 (1983) 339.
[13] R. Albrecht, Prog. Drug Res. 21 (1977) 9.
[14] J.M. Domagala, L.D. Hann, C.L. Heifetz, M.P. Hutt, T.F. Mich, J.P. Sachez, M. Solomon, J. Med. Chem. 29 (1986) 394.
[15] A. Sulkowska, M. Maciazek-Jurczyk, B. Bojko, J. Rownicka, I. Zubik-Skupien, E. Temba, D. Pentak, W.W. Sulkowski, J. Mol. Struct. 881 (2008) 97.
[16] J.Q. Lu, F. Jin, T.Q. Sun, X.W. Zhou, Int. J. Biol. Macromol. 40 (2007) 299.
[17] W.R. Wave, J. Phys. Chem. 66 (1962) 455.
[18] S.R. Knaub, M.J. Priston, M.D. Morton, J.D. Slechta, D.G. Vander Velde, C.M. Riley, J. Pharm. Biomed. Anal. 10 (1995) 1225.
[19] N. Zhang, X.L. Zhang, Y.F. Zhao, Microchem. J. 75 (2003) 249.
[20] M. Guo, Q.S. Yu, J.W. Yan, F. Tan, G.Z. Ma, Chin. Chem. Lett. 15 (2004) 1331.
[21] W. Yao, F. Gao, L. Zhang, L. Wang, J. Anal. Lab. 11 (2004) 70.
[22] J. Tang, F. Luan, X. Chen, Bioorg. Med. Chem. 12 (2006) 3210.
[23] F. Tang, X.H. Wen, M. Guo, S. Yi, G.Z. Ma, Q.S. Yu, Chin. J. Chem. 23 (2005) 37.
[24] X. Chen, J.C. Fan, Y. Wang, C.P. Fan, Z.C. Shang, Anal. Sci. 22 (2006) 427.
[25] H. He, H.Y. Ye, L. Dai, Q.C. Jiao, P.H. Chuong, Spectrosc. Sped. Anal. 26 (2006) 480.
[26] W. He, Y. Li, H. Si, Y. Dong, F. Sheng, X. Yao, Z. Hu, J. Photochem. Photobiol. A: Chem. 182 (2006) 158.
[27] S. Soetino, G. Condorelli, New J. Chem. 26 (2002) 250.
[28] A.Q. Gong, X.S. Zhu, Y.Y. Hu, S.H. Yu, Talanta 73 (2007) 668.
[29] D. Silva, C.M. Cortez, J.C. Bastos, Toxicol. Lett. 147 (2004) 53.
[30] J.R. Lakowicz, in: Principle of Fluorescence Spectroscopy, second ed., Plenum Press, New York, 1999, pp. 237–265.
[31] R.E. Mauric, A.G. Camillo, Anal. Biochem. 141 (1981) 199.
[32] T. Peters, in: All About Albumin, Academic Press, San Diego (CA), 1996.
[33] X.M. He, D.C. Carter, Nature 358 (1992) 209.
[34] G.Z. Chen, X.Z. Huang, J.G. Xu, Z.Z. Zheng, Z.B. Wang, The Methods of Fluorescence Analysis, Beijing Science Press, second ed., , 1990, pp. 2–112.

[35] J.R. Lakowicz, in: Principle of Fluorescence Spectroscopy, second ed., Kluwer/Plenum, New York, 1999.
[36] J.N. Tian, J.Q. Liu, W.Y. He, Z.D. Hu, X.Y. Yao, X.G. Chen, Biomacromolecules 5 (2004) 1956.
[37] R. Eftink, C.A. Ghiron, Anal. Chem. 114 (1982) 199–227.
[38] S.S. Lehrer, Biochemistry 10 (1971) 3254.
[39] D. Leis, S. Barbosa, D. Attwood, P. Taboada, V. Mosquera, J. Phys. Chem. B 106 (2002) 9143.
[40] A.K. Bordbar, A. Taheri-Kafrani, S.H.A. Mousavi, T. Haertle, Archiv. Biochem. Biophys. 470 (2008) 103.
[41] M.A. Cheema, P. Taboada, S. Barbosa, E. Castro, M. Siddiq, V. Mosquera, Biomacromolecules 8 (2007) 2576.
[42] F. Naseem, R.H. Khan, S.K. Haq, A. Naeem, Biochim. Biophys. Acta 1648 (2003) 115.
[43] W. Qiu, I. Zhang, O. Okobiah, Y. Yang, L. Wang, D. Zhong, A.H. Zewail, J. Phys. Chem. B 110 (2006) 10540.
[44] A. Papadopoulou, R.J. Green, R.A. Frazier, J. Agric. Food Chem. 53 (2005) 158.
[45] M.X. Xie, M. Long, Y. Liu, C. Qin, Y.D. Wang, Biochim. Biophys. Acta 1760 (2006) 1184.
[46] Y.M. Huang, Z.J. Zhang, D.J. Zhang, J.G. Lv, Talanta 53 (2001) 835.
[47] M. Jiang, M.X. Xie, D. Zheng, Y. Liu, X.Y. Li, X. Chen, J. Mol. Struct. 692 (2004) 71.
[48] H.M. Zhang, Y.Q. Wang, Q.H. Zhou, G.L. Wang, J. Mol. Struct. 921 (2009) 156.
[49] R.E. Maurice, A.G. Camillo, Anal. Biochem. 114 (1981) 199.
[50] D. Leckband, Annu. Rev. Biophys. Biomol. Struct. 29 (2000) 1.
[51] J.M. Klotz, N.Y. Ann., Acad. Sci. 226 (1973) 18.
[52] J.N. Tian, J.Q. Liu, W.Y. He, Z.D. Hu, X.G. Chen, Biomacromolecules 5 (2004) 1956.
[53] S.N. Timasheff, in: H. Peeters (Ed.), Protein of Biological Fluids, Pergamon Press, Oxford, 1972, p. 511.
[54] P.D. Ross, S. Subramanian, Biochemistry 20 (1981) 3096.
[55] T. Orster, O. Sinaoglu (Eds.), Moder Quantum Chemistry, vol. 3, Academic Press, New York, 1996.
[56] W.D. Horrocks, W.E. Collier, J. Am. Chem. Soc. 103 (1981) 2856.
[57] R.K. Nanda, N. Sarkar, R. Banerjee, J. Photochem. Photobiol. A 192 (2007) 152.
[58] Y.J. Hu, Y. Liu, Z.B. Pi, S.S. Qu, Bioorg. Med. Chem. 13 (2005) 6609.
[59] J.N. Miller, Anal. Proc. 16 (1979) 203.
[60] B. Klajnert, M. Bryszewska, Bioelectrochemistry 55 (2002) 33.
[61] S.K. Patra, A.K. Mandal, M.K. Pal, J. Photochem. Photobiol. A: Chem. 122 (1999) 23.
[62] J.B. Xiao, J. Shi, H. Cao, S.D. Wu, F.L. Ren, M. Xu, J. Pharm. Biomed. Anal. 45 (2007) 609.
[63] S. Venkateshrao, P.T. Manoharan, Spectrochim. Acta A 60 (2004) 2523.
[64] N. Sreerama, R.W. Woody, Anal. Biochem. 287 (2000) 252.
[65] H.M. Zhang, Y.Q. Wang, M.L. Jiang, Dyes Pigm. 82 (2009) 156.
[66] S. Georgakopoulu, D. Moller, N. Sachs, H. Herrmann, U. Aebi, J. Mol. Biol. 386 (2009) 544.
[67] S. Era, K.B. Itoh, M. Sogami, K. Kuwata, T. Iwama, H. Yamada, H. Watari, Int. J. Pept. Protein Res. 35 (1990) 1.
[68] A. Pedretti, L. Villa, G. Vistoli, J. Mol. Graph. 21 (2002) 47.
[69] G. Morris, in: SYBYL Software, Version 6.9, Tripos Associates Inc, St. Louis, 2002.
[70] R.J. Rosenfeld, D.S. Goodsell, R.A. Musah, G.M. Morris, D.B. Goodin, A.J. Olson, J. Comput. Aided Mol. Des. 17 (2003) 525.